

is believed that carrier-mediated ferromagnetism in the II-IV- V_2 chalcopyrites is favored when Mn occupies the group-IV site, where it is likely to be electrically active¹⁶. For this reason we first explore the competition between substitutional Mn doping on the II and IV sites by computing the Mn impurity formation energy on each site. Second, we address whether occupation of the group-IV sites is indeed likely to lead to a ferromagnetic phase; in particular, for each host we compute the Heisenberg spin coupling for an experimentally reasonable Mn concentration. The magnitude (and sign) of this coupling should serve as a useful roadmap for the experimental exploration of new ferromagnetic chalcopyrites.

Of the 64 chalcopyrites considered here, about 1/3 are known to exist and have been studied experimentally. A few crystallize in both the chalcopyrite and sphalerite structure (e.g. $CdGeP_2$ and $ZnSnSb_2$), while two take the wurzite structure ($BeSiN_2$ and $ZnGeN_2$); for simplicity we treat all 64 in the chalcopyrite structure. For those with measured lattice parameters, we can compare our theoretical predictions. As expected from DFT calculations, a is given very accurately (within $\sim 1\%$), while c is less so ($\lesssim 15\%$). As Fig. 1 shows, nearly half of the 64 chalcopyrites enjoy a close lattice match to an important mainstream semiconductor.

As with all semiconductors, DFT in the generalized-gradient approximation significantly underestimates band gaps. For chalcopyrites whose measured gaps are in the range 1–2 eV, the DFT values are approximately 1 eV smaller than measured, consistent with previous findings¹⁷. Hence the theoretical gaps shown in Fig. 1 must be viewed with caution: the true gaps are likely to be at least 1 eV larger than predicted. Likewise, hosts that have no gap within DFT may in reality have a gap (which is likely to be 1 eV or smaller). These caveats aside, the trend in Fig. 1 is standard for covalently bonded semiconductors: smaller lattice constants are associated with larger band gaps. In particular, the nitrides have the smallest lattice constants and largest gaps, while the antimonides have the largest lattice constants and smallest gaps. From the perspective of our survey, the range and distribution of lattice constants and band gaps is satisfyingly large, guaranteeing our roadmap good coverage of this unexplored territory.

Not all of the chalcopyrites considered here are thermodynamically stable, even in the absence of Mn. Fig. 2 shows the calculated enthalpies of formation, $\Delta H_f(\text{II-IV-}V_2) = E(\text{II-IV-}V_2) - E(\text{II}) - E(\text{IV}) - 2E(V)$, where the latter terms refer to the ground-state elemental phases. Of the 64 chalcopyrites, 3/4 have negative enthalpies, suggesting many potentially stable host materials. (We have not considered phase stability with respect to disproportionation into compound products, and so the terms “stable” and “unstable” should be understood here with this caveat.) The trend in Fig. 2 is similar, and indeed intimately related, to that of Fig. 1: smaller lattice constants are usually associated with higher stability. Hence, as expected, the nitrides tend to be the

most stable chalcopyrites and the antimonides the least stable. Note that there are important deviations from this trend: for example, nearly all the carbides are unstable.

The solubility of Mn in a host chalcopyrite is an extremely important issue for two reasons. The first pertains to the well-known tendency, within Mn-doped DMS materials, toward phase separation with increasing Mn content^{1,2}. This tendency is reflected in the very low equilibrium solubility limit of Mn in, for example, III-V hosts—typically of order parts per thousand or less. These limits can be greatly exceeded, by 2–3 orders of magnitude, by relying on kinetic barriers to maintain the metastable phase. It is not feasible to address this issue theoretically for the chalcopyrites. Instead, we propose using the theoretical solubility limit of Mn as a rough proxy for the metastability doping limit. The solubility limit of Mn, x_{sol} , is determined by its impurity formation energy, $\Delta H_f(\text{Mn})$, simply according to $x_{\text{sol}} = \exp(-\Delta H_f(\text{Mn})/kT)$. In this formulation, a negative formation energy implies that spontaneous incorporation of Mn impurities will be limited only by kinetics¹⁸.

The second reason concerns ferromagnetism per se. In general, the solubility limits for Mn substituting on the group-II and -IV sites will be different. Mahadevan and Zunger have shown that, in the case of $CdGeP_2$, substitutional Mn_{II} leads to antiferromagnetic interactions while Mn_{IV} leads to ferromagnetic interactions¹⁶. Hence the II-IV solubility difference will greatly influence the stability, or even existence, of the ferromagnetic phase, as well as the attainable Curie temperatures. There are two other important issues, which we do not address here. One is the possibility of Mn occupying interstitial sites (which is increasingly likely for hosts with small lattice constants¹⁹) or forming complexes with other Mn or native defects; if electrically active, these can have consequences for ferromagnetism. The other is the possibility

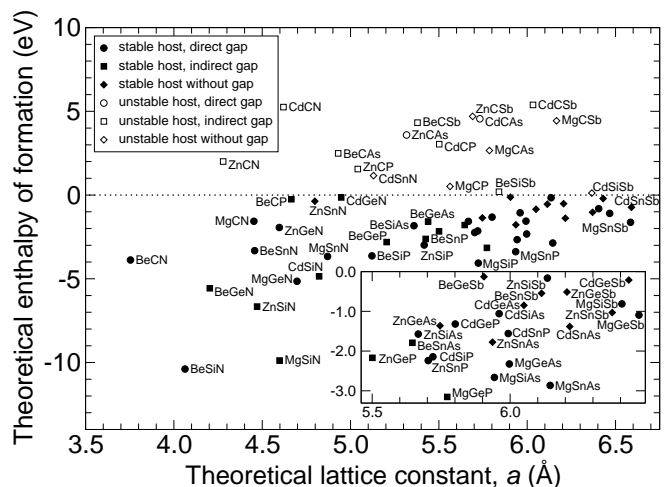


FIG. 2: Theoretical enthalpy of formation vs. lattice constant for II-IV- V_2 chalcopyrites. Negative enthalpy implies a stable host compound.

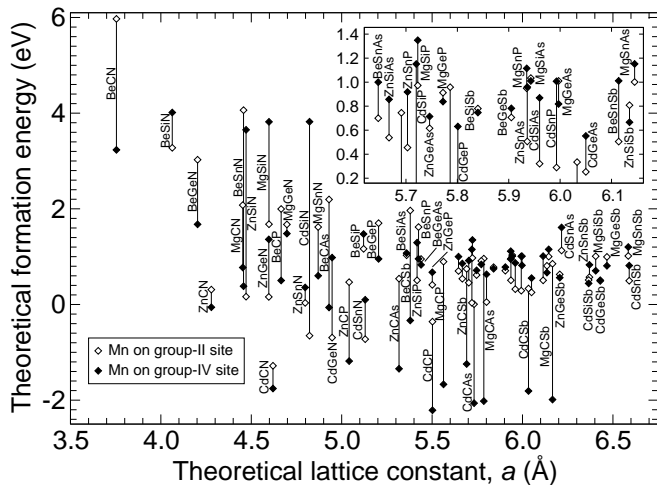


FIG. 3: Theoretical impurity formation energy of substitutional Mn vs. lattice constant of host chalcopyrite. Chemical potentials were defined by assuming the simultaneously II-rich and IV-rich condition.

that even substitutional Mn may be subject to a Jahn-Teller distortion, which can affect the magnetic interactions as discussed in Ref. [20].

It is important to realize that the impurity formation energy (and hence the solubility limit) in a multicomponent host is not uniquely defined, but depends on the growth environment—in particular, on the energy μ required to transfer one atom from a reservoir into the host compound²¹. For the ternary chalcopyrites there are three such chemical potentials, $\{\mu_{\text{II}}, \mu_{\text{IV}}, \mu_{\text{V}}\}$, which are related by $\mu_{\text{II}} + \mu_{\text{IV}} + 2\mu_{\text{V}} = \Delta H_f(\text{II-IV-V}_2)$. The formation energies shown in Fig. 3 were evaluated for μ_{II} and μ_{IV} at their highest allowed values, corresponding to a simultaneously II-rich and IV-rich growth environment. This condition can often be realized experimentally, unless a more stable compound intervenes. With this choice, half of the chalcopyrite hosts (including all of the carbides) prefer Mn on the group-II site, while half (including most of the silicides) prefer the group-IV site. For both the II and IV sites, there is the expected trend of larger lattice constants leading to smaller impurity formation energies—and hence to higher solubilities. This trend begins to disappear for lattice constants larger than ~ 6 Å; in this regime there is enough room available for the Mn impurity that the formation energies become essentially independent of both site and host.

In the remainder of this work we assume that the prospects for ferromagnetism are best served when Mn substitutes on the group-IV site¹⁶. The doping can be biased in this direction by changing the growth environment to the simultaneously II-rich and IV-poor condition, which reduces the relative Mn_{IV} formation energy, $\Delta E = \Delta H_f(\text{Mn}_{\text{IV}}) - \Delta H_f(\text{Mn}_{\text{II}})$, to its minimum physically allowed value. The magnitude of the reduction depends on the nature of other possible intervening phases $\text{II}_x\text{IV}_y\text{V}_z$, which we do not pursue here (see Ref. [22] for

a related discussion). In the best-case scenario, the limiting IV-poor condition will lead to a change in ΔE by an amount $\Delta H_f(\text{II-IV-V}_2)$, relative to the values shown in Fig. 3. Using our calculated enthalpies, we find this limiting IV-poor condition favors Mn on the group-IV site in 50 of the 64 hosts (the carbides are again the dominant exception). Thus we conclude that under suitable growth conditions, substitutional Mn can be forced to preferentially occupy the group-IV site in the majority of chalcopyrite hosts.

Even in such favorable cases, one expects some fractional occupation of Mn on group-II sites. Since this doping is isoelectronic it is unlikely to produce either holes or electrons, and thus will probably require additional doping to order ferromagnetically. A more pressing question is whether Mn doping on the group-IV sites necessarily leads to ferromagnetism in every II-IV-V₂ chalcopyrite. And, for those hosts that can be made ferromagnetic, it is of great interest to know what Curie temperatures one can expect.

These are very difficult questions to address comprehensively, in a materials-specific framework, for any random magnetic alloy. Instead, we adopt again our earlier view and focus on a simple proxy for ferromagnetism, namely the nearest-neighbor Heisenberg coupling, J , for a specific distribution of Mn in each host. In the mean-field theory of Heisenberg ferromagnetism, the Curie temperature is simply proportional to $|J|$, with a proportionality constant depending on the spatial distribution of Mn. Nevertheless, we caution that while qualitative trends in J are likely to be meaningful within this materials class, the quantitative prediction of Curie temperatures in ferromagnetic semiconductors remains a difficult problem. Here we choose a fixed, experimentally reasonable Mn concentration of 12.5% (see, for example, Ref. [11]), and examine how J varies across different hosts. In a related study of the I-III-VI₂ chalcopyrite CuGaSe_2 , Picozzi *et al.* showed that $|J|$ increases with Mn concentration²³. Our method for computing J is the same as in Ref. [23], and gives nearly identical results for CuGaSe_2 with 12.5% Mn.

Surprisingly, we find that ferromagnetic alignment is favored (J is negative) in only half of the 64 chalcopyrites. Three main factors determine the behavior of J across different hosts. The first is the group-II element: the majority of Mg- and Cd-containing hosts favor ferromagnetic alignment, while the majority of Be- and Zn-containing hosts favor antiferromagnetic alignment. The second factor is the group-IV element: for many combinations of II and V elements, we find the ordering $J(\text{C}) < J(\text{Si}) < J(\text{Ge}) < J(\text{Sn})$, except in the nitrides (see Supplementary Information, Fig. S1). The group-V element plays the third—and lesser—role, with the ordering $J(\text{P}) < J(\text{As}) < J(\text{Sb})$ obtained for most cases except the carbides (see Supplementary Information, Fig. S2). None of these trends can be attributed to the approximate scaling, $J \sim a^{-3}$, predicted by the mean-field solution of the Zener model²⁴; indeed, across

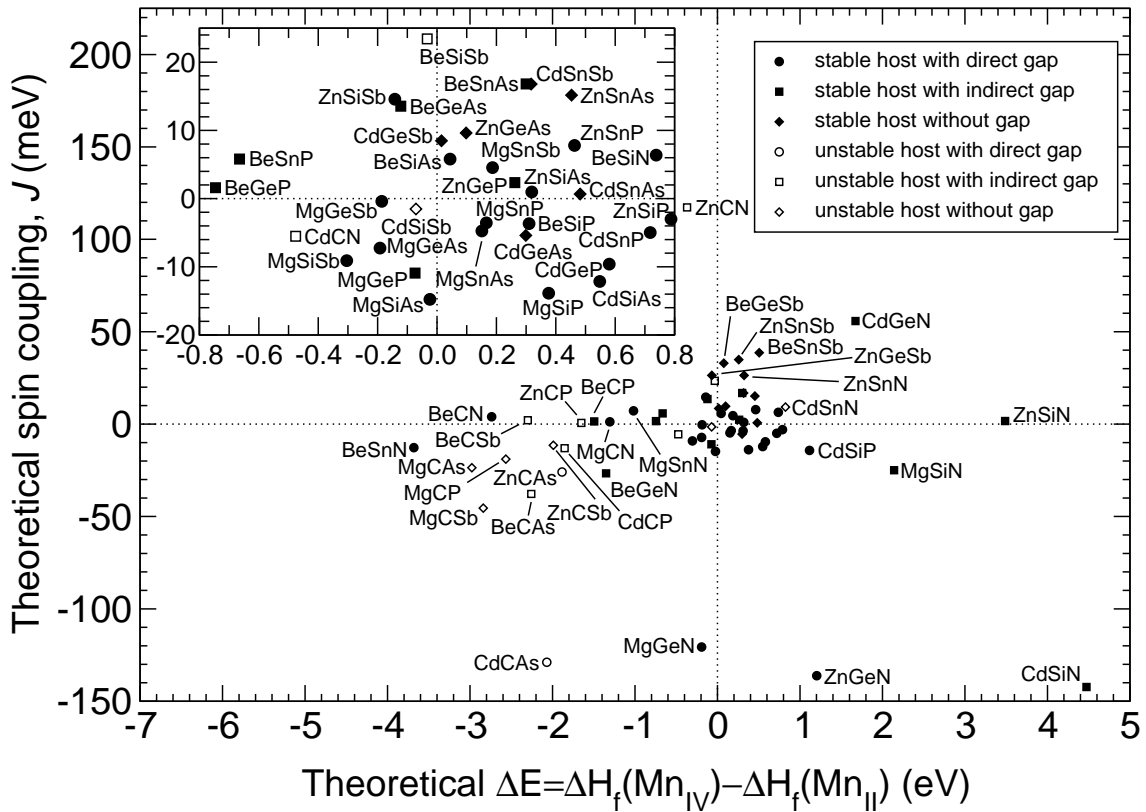


FIG. 4: Theoretical spin coupling between Mn_{IV} vs. relative impurity formation energy of Mn_{IV} . Negative spin coupling implies ferromagnetic ordering is favored; negative ΔE implies substitutional Mn on the group-IV site is favored. Chemical potentials were defined by assuming the simultaneously II-rich and IV-rich condition. One host, $CdCSb_2$, falls outside the plot range ($\Delta E = -2.1$ eV, $J = -350$ meV) but is thermodynamically unstable.

this class of chalcopyrites we find no universal dependence of J on lattice constant (see Supplementary Information, Fig. S3). Nor do we find any simple correlation between J and the bandgap; such a correlation might have been expected if the small-gap hosts reflected Zener physics (with modest Curie temperatures) and the large-gap hosts double-exchange physics (with higher Curie temperatures)²⁵.

Fig. 4 shows the computed values of J plotted against the relative Mn_{IV} impurity formation energy, ΔE . We do not imply any correlation between these two quantities, but rather display them together because each is centrally important for designing new ferromagnetic chalcopyrites. In particular, the lower-left quadrant contains chalcopyrites for which occupation by, and ferromagnetic alignment of, Mn on the group-IV site is favorable under experimentally plausible II- and IV-rich growth conditions. This conservatively defined sweet spot contains just 19 chalcopyrites out of the full set of 64. Of these, only eight are thermodynamically stable: four are lattice-matched to a mainstream semiconductor ($BeSnN_2$, $MgGeP_2$, $MgSiAs_2$, $MgGeAs_2$) and four are not ($BeGeN_2$, $MgSiSb_2$, $MgGeN_2$, $MgGeSb_2$). Seven of these eight have values of J comparable to, or larger than, that of $CdGeP_2$ and thus can be expected to have

similar Curie temperatures—of order room temperature or larger. This small set of materials should provide a propitious starting point for more detailed experimental and theoretical scrutiny.

One can also consider the best-case scenario described earlier and consider ΔE in the limiting IV-poor growth condition. This leads to horizontal shifts, by ΔH_f , of the points in Fig. 4—leftward for negative enthalpies and rightward for positive—and thereby moves 13 more chalcopyrites into the lower left sweet spot. Ten of these are lattice-matched to mainstream semiconductors ($MgSiN_2$, $MgSiP_2$, $MgSnP_2$, $MgSnAs_2$, $ZnSiP_2$, $ZnGeN_2$, $CdSiP_2$, $CdSiAs_2$, $CdGeAs_2$, $CdSnP_2$), and three are not ($BeSiP_2$, $CdSiN_2$, $CdGeP_2$); all are thermodynamically stable.

Experimentally, $CdGeP_2$ and $ZnSnAs_2$ have ferromagnetic ground states with comparable Curie temperatures, while $ZnGeP_2$ has an antiferromagnetic ground state (ferromagnetism disappears below 47 K [11]). Our results, which presume Mn doping on the group-IV site, predict $CdGeP_2$ to be ferromagnetic but $ZnSnAs_2$ and $ZnGeP_2$ to be antiferromagnetic. Reconciling these findings is problematic, because the experimental group-II and -IV chemical potentials—and thereby the favored Mn site—are in general not known. The available evidence points to Mn_{IV} substitution in $CdGeP_2$ [16], Mn_{II} in $ZnGeP_2$

[11], and mixed occupation in ZnSnAs_2 [12]. Future work addressing the magnetic interactions between Mn on group-II sites is in progress.

Finally, we address the prospects for using ferromagnetic chalcopyrites as sources of spin-polarized current for injection into nonmagnetic semiconductors. Many issues play a role in this process, including the spin polarization of states at the Fermi level, the band velocities of those states, native defects and other structural inhomogeneities, and spin scattering at the interface³. Here we focus on the first of these. For dilute Mn doping (12.5% and 6.25%, and presumably below this as well), all of the 21 stable ferromagnetic chalcopyrites identified above are “idealized half-metals,” by which we mean that at zero temperature and for an ordered arrangement of Mn, there are states at the Fermi level only in one spin channel. The effects of both finite temperature and site disorder will generally reduce the spin polarization from this idealized case. At higher Mn concentration (50%), half-metallicity persists for all but two of these 21 hosts (BeSnN_2 , CdSiN_2). Even when Mn completely occupies the group-IV sublattice, the resulting stoichiometric compounds are half-metallic in all cases except for the nitrides. Thus the prospects for using ferromagnetic chalcopyrites as spin-polarized sources appear quite favorable.

In summary, we have examined theoretically the prospects for ferromagnetism within the class of all possible II-IV-V₂ chalcopyrites having constituents chosen from the first four rows of the Periodic Table. As expected for semiconductors, we find that the electronic properties of the host materials (band gap and enthalpy of formation) are closely related to their structural properties (lattice constant, a). Contrary to conventional wisdom, we do not find that Mn is generally more soluble on the group-II site than on the group-IV site; instead, the relative site solubility depends on both the nature of the host (e.g. carbide vs. silicide) and the choice of growth condition, while the absolute Mn solubility is largely determined by the host lattice constant. Our results for the Heisenberg coupling between Mn show that the Curie temperatures expected in Mn-doped chalcopyrites do not follow the scaling with lattice constant predicted by the Zener model; nor do they show any systematic variation with band gap, as the double-exchange model would predict. By identifying those chalcopyrites that simultaneously exhibit thermodynamic stability, favorable Mn doping site, and ferromagnetic Mn interactions, we iden-

tify two small sets of chalcopyrites that show excellent prospects for stable ferromagnetism under realistic and attainable experimental conditions.

This work was supported by ONR and the DARPA SpinS program. I.Ž. acknowledges financial support from the National Research Council. Discussions with G.A. Medvedkin are gratefully acknowledged. Computations were performed at the DoD Major Shared Resource Center at ASC.

Methods. All the numerical results reported here are based on density-functional theory in the generalized-gradient approximation¹³, using ultrasoft pseudopotentials as implemented in VASP^{14,15}. For each host chalcopyrite, the plane-wave cutoff was separately determined by the three constituent elements (four if Mn was included). For the undoped hosts, equilibrium lattice parameters and the internal coordinate were optimized using a $4\times 4\times 4$ Monkhorst-Pack sampling of the Brillouin zone. Band gaps were evaluated by identifying band edges based on a $12\times 12\times 12$ sampling that included the zone center and high-symmetry points.

For enthalpies of formation, the total energies of the elemental phases were calculated using the following structures, which are either ground-state phases or energetically very close thereto: hcp (Be, Mg, Cd, Zn); diamond (C, Si, Ge); white-tin (Sn); molecular dimer (N); black phosphorous (P); αAs (As, Sb).

Mn impurity formation energies were computed using simple cubic (or, for non-ideal c/a , tetragonal) supercells of 64 host atoms. To properly represent the dilute impurity limit, all atomic positions were relaxed with fixed ideal supercell lattice parameters, within the constraint that Mn remain on-center. A single Monkhorst-Pack k -point was used. Chemical potentials were defined with respect to their thermodynamic upper limit determined by the elemental phases listed above. For the Mn chemical potential, a non-magnetic fcc structure was used to approximate the more complicated αMn ground-state phase.

Heisenberg spin couplings for 12.5% Mn-doped chalcopyrites were computed using the method described in Ref. 23. The lattice parameters and internal coordinate of each supercell were assumed to depend linearly on the Mn content (Vegard’s law), and were interpolated using lattice parameters and internal coordinate calculated for the fully Mn_{IV}-substituted host. Two Mn per 64-atom supercell were then arranged on a uniform lattice and full atomic relaxation was performed. Total energies for two spin configurations were computed—ferromagnetic, and antiferromagnetic with [100] ordering wavevector—whereupon the energy difference gives J within the nearest-neighbor Heisenberg model.

1. Ohno, H. Making nonmagnetic semiconductors ferromagnetic. *Science* **281**, 951–956 (1998).
 2. Maekawa, S. and Shinjo, T. (Eds.). *Spin Dependent Transport in Magnetic Nanostructures*. Taylor and Francis, New York, (2002).
 3. Žutić, I., Fabian, J., and Das Sarma, S. Spintronics: Fundamentals and applications. *Rev. Mod. Phys.* **76** (2004).

(in press).

4. Dietl, T. Functional ferromagnetics. *Nature Mater.* **2**, 646–648 (2003).
 5. Dietl, T., Ohno, H., Matsukura, F., Cibert, J., and Fermand, D. Zener model description of ferromagnetism in zinc-blende magnetic semiconductors. *Science* **287**, 1019 (2000).

6. König, J., Lin, H.-H., and MacDonald, A. H. Theory of diluted magnetic semiconductor ferromagnetism. *Phys. Rev. Lett.* **84**, 5628–5631 (2000).
7. Chattopadhyay, A., Das Sarma, S., and Millis, A. J. Transition temperature of ferromagnetic semiconductors: a dynamical mean field study. *Phys. Rev. Lett.* **87**, 227202 (2001).
8. Nagaev, E. L. *Colossal Magnetoresistance and Phase Separation in Magnetic Semiconductors*. Imperial College Press, London, (2002).
9. Medvedkin, G. A., Ishibashi, T., Hayata, T. N., Hasegawa, Y., and Sato, K. Room temperature ferromagnetism in novel diluted magnetic semiconductor $\text{Cd}_{1-x}\text{Mn}_x\text{GeP}_2$. *Jpn. J. Appl. Phys., Part 2* **39**, L949–951 (2000).
10. Medvedkin, G. A., Hirose, K., Ishibashi, T., Nishi, T., Voevodin, V. G., and Sato, K. New magnetic materials in ZnGeP_2Mn chalcopyrite system. *Journal of Crystal Growth* **236**, 609–612 (2002).
11. Cho, S., Choi, S., Cha, G.-B., Hong, S. C., Kim, Y., Zhao, Y.-J., Freeman, A. J., Ketterson, J. B., Kim, B. J., and Kim, Y. C. Room-temperature ferromagnetism in $\text{Zn}_{1-x}\text{Mn}_x\text{GeP}_2$ semiconductors. *Phys. Rev. Lett.* **88**, 257203 (2002).
12. Choi, S., Cha, G.-B., Hong, S. C., Cho, S., Kim, Y., Ketterson, J. B., Jeong, S.-Y., and Yi, G. C. Room-temperature ferromagnetism in chalcopyrite Mn-doped ZnSnAs_2 single crystals. *Solid State Comm.* **122**, 165–167 (2002).
13. Perdew, J. P., Chevary, J. A., Vosko, S. H., Jackson, K. A., Pederson, M. R., Singh, D. J., and Fiolhais, C. Atoms, molecules, solids, and surfaces: Applications of the generalized gradient approximation for exchange and correlation. *Phys. Rev. B* **46**, 6671–6687 (1992).
14. Kresse, G. and Hafner, J. Ab initio molecular dynamics for liquid metals. *Phys. Rev. B* **47**, 558–561 (1993).
15. Kresse, G. and Furthmüller, J. Efficient iterative schemes for ab initio total-energy calculations using a plane-wave basis set. *Phys. Rev. B* **54**, 11169–11186 (1996).
16. Mahadevan, P. and Zunger, A. Room-temperature ferromagnetism in Mn-doped semiconducting CdGeP_2 . *Phys. Rev. Lett.* **88**, 047205 (2002).
17. Continenza, A., Massidda, S., Freeman, A. J., de Pascale, T. M., Meloni, F., and Serra, M. Structural and electronic properties of narrow-gap ABC_2 chalcopyrite semiconductors. *Phys. Rev. B* **46**, 10070–10077 (1992).
18. Zhang, S. B. The microscopic origin of the doping limits in semiconductors and wide-gap materials and recent developments in overcoming these limits: a review. *J. Phys.: Condens. Matter* **14**, R881–R903 (2002).
19. Erwin, S. C. and Hellberg, C. S. Predicted absence of ferromagnetism in manganese-doped diamond. *Phys. Rev. B* **68**, 245206 (2003).
20. Kacman, P. Spin interactions in diluted magnetic semiconductors and magnetic semiconductor structures. *Semicond. Sci. Technol.* **16**, R25–R39 (2001).
21. Van de Walle, C. G., Limpijumnong, S., and Neugebauer, J. First-principles studies of beryllium doping of GaN. *Phys. Rev. B* **63**, 245205 (2001).
22. Zhao, Y.-J. and Zunger, A. Site preference for Mn substitution in spintronic $\text{CuM}^{\text{III}}\text{X}_2^{\text{VI}}$ chalcopyrite semiconductors. *Phys. Rev. B* **69**, 075208 (2004).
23. Picozzi, S., Zhao, Y.-J., Freeman, A. J., and Delley, B. Mn-doped CuGaS_2 chalcopyrites: an ab initio study of ferromagnetic semiconductors. *Phys. Rev. B* **66**, 205206 (2002).
24. Dietl, T., Ohno, H., and Matsukura, F. Hole-mediated ferromagnetism in tetrahedrally coordinated semiconductors. *Phys. Rev. B* **63**, 195205 (2001).
25. Pearton, S. J., Abernathy, C. R., Overberg, M. E., Thaler, G. T., Norton, D. P., Theodoropoulou, N., Hebard, A. F., Park, Y. D., Ren, F., Kim, J., and Boatner, L. A. Wide band gap ferromagnetic semiconductors and oxides. *J. Appl. Phys.* **93**, 1–13 (2003).

Supplement

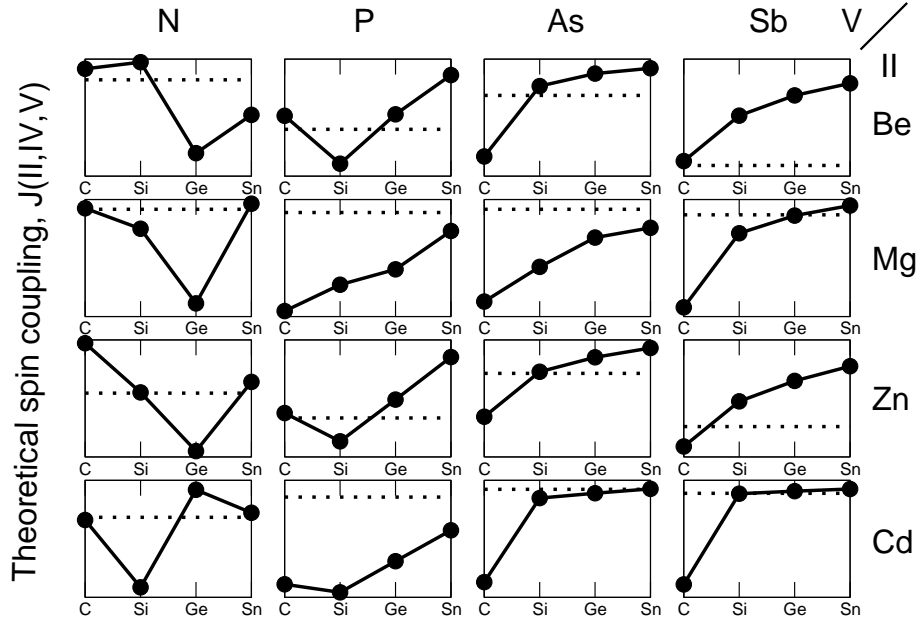


FIG. 5: [FIG. S1] Theoretical Mn_{IV} spin coupling vs. group-IV element, for each of 16 sets of II-IV- V_2 chalcopyrites. Results are plotted with arbitrary units to emphasize trends; the dotted lines denote $J = 0$. For many combinations of II and V elements, the ordering $J(C) < J(Si) < J(Ge) < J(Sn)$ is found, except in the nitrides.

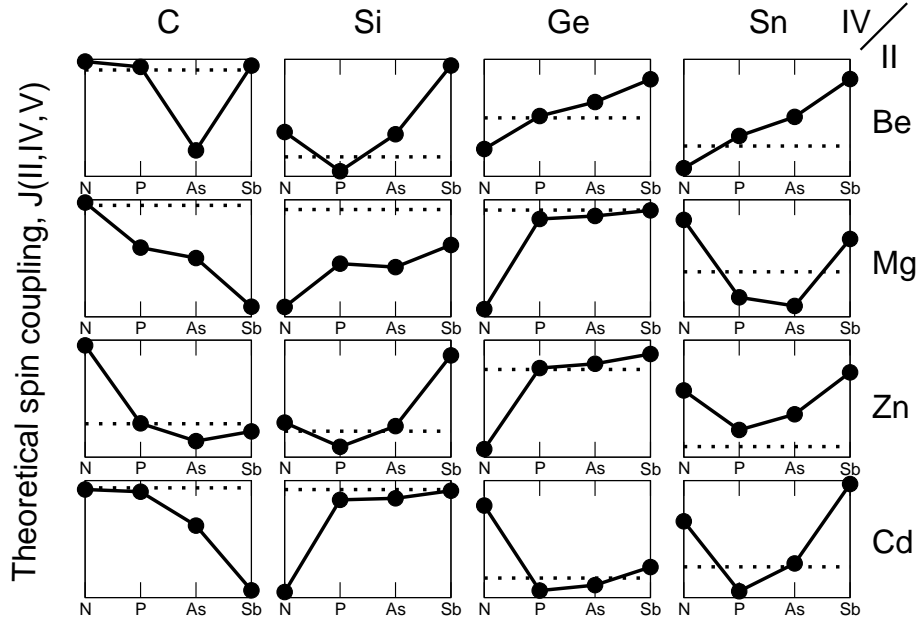


FIG. 6: [FIG. S2] Theoretical Mn_{IV} spin coupling vs. group-V element, for each of 16 sets of II-IV- V_2 chalcopyrites. Results are plotted with arbitrary units to emphasize trends; the dotted lines denote $J = 0$. The ordering $J(P) < J(As) < J(Sb)$ is obtained for most cases, except in the carbides.

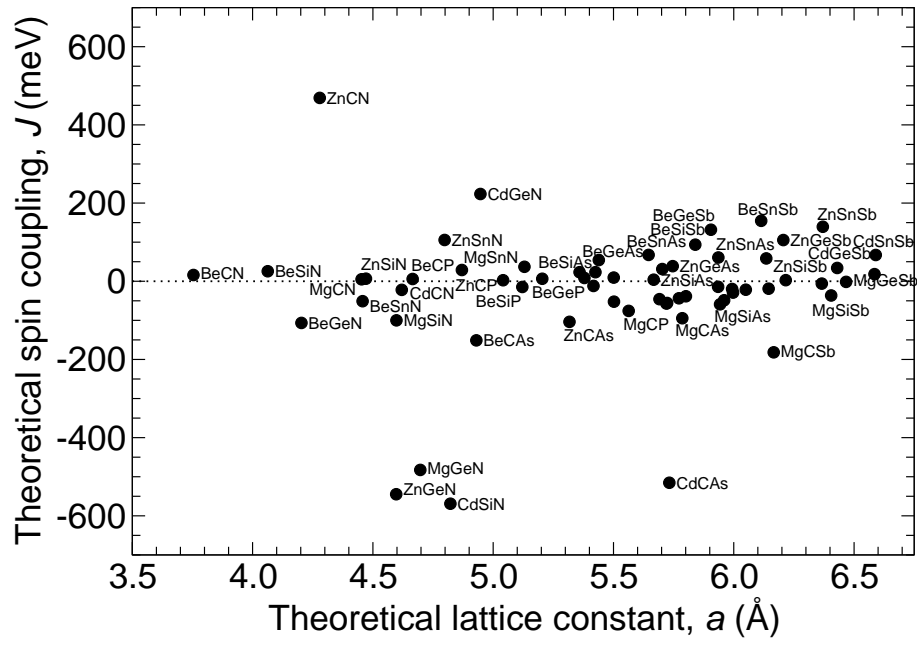


FIG. 7: [FIG. S3] Theoretical Mn_{IV} spin coupling vs. lattice constant of host chalcopyrite. No evidence is observed for the approximate scaling, $J \sim a^{-3}$, predicted by the mean-field solution of the Zener model.